EXPERIMENTAL INVESTIGATION OF LOW TEMPERATURE COMBUSTION IN A DIESEL ENGINE DEPENDING ON INJECTION ADVANCE AND INJECTION PRESSURE

by

Onur GEZER*, Orkun OZENER, and Muammer OZKAN

Department of Mechanical Engineering, Yildiz Technical University, Istanbul, Turkey

Original scientific paper
https://doi.org/10.2298/TSCI240105155G

In this study, the performance parameters and emissions of a pre-mixed charge compression ignition were investigated under different injection pressures and injection advances. After the peak engine power was reached, reasonable decreases occurred in brake mean effective pressure at certain injection advances with the increase of injection advance, and dramatic decreases observed when interval was so exceeded. In addition mean indicated pressure and peak in-cylinder pressure were investigated. Considering the emissions, dramatic increases were observed in CO and total hydrocarbon, depending on the increase in the low temperature combustion regime. The NO_x started a rapid downward trend after a certain injection advance value in the experimental region, but this effect did not occur at the desired level for specific NO_x. It was observed that the NO_2 to NO_x ratio increased as the pre-mixed charge compression ignition became dominant and NO_2 production increased among the total NO_x. In the operating region where the low temperature combustion regime was dominant, the targeted reduction in NO_x and particulate matter emissions was observed, but the desired reduction in specific emissions did not occur. In the low temperature combustion region, the combustion process was prolonged, initially reasonable changes occurred at performance parameters, but unacceptable results were observed at high injection pressures with excessive injection advances.

Key words: *low temperature combustion, pre-mixed charge compression ignition, emission, performance, diesel combustion*

Introduction

Controlling NO_x and particulate matter (PM) simultaneously is quite difficult in a conventional diesel combustion (CDC) due to trade-off formation mechanisms. NO_x increases at high temperature [1], especially at lean mixtures above 2200 K, while PM increases dramatically at rich mixture above 1800 K [2]. If fuel is injected earlier, the mixing process starts under lower pressure and temperature. At this moment, fuel jet penetration depth increases due to lower ambient pressure and lower resistance to movement, so fuel droplets spread to a much more volume. Moreover, the lower ambient temperature and lower turbulence level leads to an increase in the fuel droplet break-up duration. Thus, fuel spreads into a larger volume. This reduces the cold zones in the combustion chamber where fuel is practically absent. Thus, the heterogeneity of the mixture, which is extremely dominant in CDC, gets reduced. As a result, leaner combustion occurs and combustion temperature decreases. This combustion strategy,

* Corresponding author, e-mail: ogezer@yildiz.edu.tr

which avoids relatively high temperature, is called as low temperature combustion (LTC) [3]. Compared to CDC, both of NO_x and PM reduce in LTC [4] due to the higher pre-mixing ratio and lower combustion temperature. The long ignition delay (ID) in LTC suppresses PM by increased homogeneity of the mixture [5].

Homogeneous charge compression ignition (HCCI), pre-mixed charge compression ignition (PCCI) and reactivity controlled compression ignition (RCCI) are three main LTC methods for diesel engines [6]. In RCCI, high octane and low cetane fuel is injected outside of cylinder or at the early moment of cycle and then diesel fuel is used as a combustion trigger. In HCCI, fuel is injected into the cylinder quite early during compression. At this moment wall wetting tendency is high and it is difficult to control the start of combustion (SOC) at this regime, so HCCI can be applied at limited low engine loads. These problems make PCCI a more attractive [7]. The PCCI can be considered as a hybrid application of HCCI and CDC [8]. The PCCI can be described as a combination of the mixture-controlled SOC of CDC and the reaction-controlled SOC of HCCI [9]. In PCCI, injection advance (IA) is between CDC and HCCI. Thus, SOC is more predictable. In PCCI, PM, and NO_x are higher than HCCI, but lower than CDC [10]. The PCCI reduces NO_x and PM simultaneously while total unburned hydrocarbon (THC) and CO increase. The PCCI is largely applied at partial loads, because complex combustion control issues have not been fully overcome [11]. Murcak *et al.* [12] observed significant power decrease with increasing IA at high loads. Similarly, Bhave *et al.* [13] changed IA between 30° CA and 45° CA bTDC and attained non-harmonious results when 50% engine load was exceeded. Nevertheless, PCCI is generally viable up to 40-50% engine load. But strong diesel knock occurs at higher engine loads [14]. The PCCI leads to prolongation of ID, decrease in burning velocity and heat release rate, lengthening of combustion duration, decrease in brake mean effective pressure (BMEP) and indicated mean effective pressure (IMEP). The results of some studies were carried out on PCCI were presented in the following paragraphs.

Qui *et al.* [15] worked at 1500 rpm, 100 MPa injection pressure (IP), 25% EGR – exhaust gas re-circulation, 0.43 MPa, and 0.86 MPa BMEP. According to results which carried out at 3° CA bTDC and 18° CA bTDC IA, the effect of IA on the ID was relatively low at high load, while differences at low load were more visible. Terragosa *et al.* [11] kept IP constant at 800 bar and changed IA between 18° CA bTDC and 38° CA bTDC. It was observed that as IA increased, peak in-cylinder pressure decreased, whereas the highest instantaneous pressure before TDC increased, to the contrary $dP/d\alpha$ decreased. Liu *et al.* [16] carried out a study at IA varied between 65° CA bTDC and 5° CA aTDC. They saw that combustion efficiency decreased at IA greater than 30° CA bTDC, while the decrease in combustion efficiency took a dramatic value around 50° CA bTDC. Nearly, 15° CA ID was observed at 35° CA bTDC IA and 55° CA at 65° CA bTDC. In other words, the excessive IA retarded the SOC. Wei *et al.* [17] conducted a study at 1800 rpm, 30% load and 110 MPa IP by varying IA between 2.5° CA bTDC and 25° CA bTDC. It was observed that peak in-cylinder pressure increased as IA increased. For boundary IA, these values were around 6 MPa and 10 MPa. The ID was the lowest at 12.5° CA bTDC and 15° CA bTDC IA. While brake thermal efficiency (BTE) was 35% at 12.5° CA bTDC IA, it decreased to 31% at 25° CA bTDC. In the study of Wei *et al.* [17], the peak in-cylinder pressure increased with increasing of IA, this indication leads to inconsistent results with Terragosa *et al.* [11], so it would be useful to gain knowledge to the literature on this subject.

Kim *et al.* [18] kept the engine load at 0.45 MPa IMEP, 40 MPa IP, 60% EGR, and IA was varied between 18° CA bTDC and 40° CA bTDC. According to results, THC was the lowest at 20°-26° CA bTDC and THC increased from this range at both sides, especially after 32° CA bTDC. The NO_x was so close at 20°-26° CA bTDC band, but a slight increase aroused

as IA decreased and a higher decreasing ratio occurred as IA increased. The PM was high below 20° CA bTDC IA, a strong decrease in PM occurred with increasing IA. Parks *et al.* [19] worked at 2.6 bar BMEP and different EGR ratio. In the study, more than 80% of NO_x reduction was occurred in PCCI compared to CDC, while CO increased as 200% and THC increased as 50%, approximately. Lui *et al.* [20] conducted a study at 0.73 MPa BMEP, 30% EGR, 100 MPa IP, IA was varied between TDC and 20° CA bTDC. Regular decreases in total PM was observed at greater than 5° CA bTDC IA, particularly rapid up to 16 ° CA bTDC. When PM diameter distributions were examined, 55 nm mean diameter was observed where start of injection (SOI) occurred at TDC, 70 nm 5° CA bTDC, and 60 nm at 13° CA bTDC, 32-33 nm at 16° CA bTDC and 26-27 nm at 20° CA bTDC, respectively. Rohani *et al.* [21] carried out a study at 30 mg per stroke injected fuel quantity (IFQ), 160 MPa IP, 60% EGR, IA varied between 20° CA bTDC and 40° CA bTDC. According to the results, IMEP was 0.54 MPa at 20° CA bTDC IA, 0.56 MPa at 25° CA bTDC, 0.57 MPa at 30° CA bTDC, 0.57 MPa at 35° CA bTDC, 0.57 MPa at 40° CA bTDC. THC was around 250 ppm at 25° CA bTDC and 30° CA bTDC IA and these values were the smallest value of investigation region, this value reached 350 ppm at 40° CA bTDC IA. The NO_x was 10 ppm at 20° CA bTDC IA, it increased to 80 ppm at 30° CA bTDC, then decreased to 20 ppm at 40° CA bTDC.

It is seen that most of the PCCI studies were conducted with high EGR [22-25]. The EGR dilutes working mixture and reduces burning rate, so EGR is desirable for PCCI. However, high EGR affects sensitivity of other combustion parameters adversely. Pandey *et al.* [26] showed that if EGR increases, ID differences decrease and become more indistinct. The effects of parameters that will directly affect the combustion, like IP and IA, are suppressed due to high EGR. For this reason, the studies carried out without EGR are presented below.

Park *et al.* [27] injected the fuel at 500 bar, 14 mg per stroke IFQ, and 3° CA increments between TDC and 27° CA bTDC IA. It was observed that the difference between IMEP and BMEP increased at higher IA. The highest in-cylinder peak pressure was observed at 27° CA bTDC IA. The THC was the lowest, as 5 ppm, at 15° CA bTDC IA, and this value increased to 35 ppm at 27° CA bTDC. The CO also showed a similar trend. The PM was the highest at 5° CA bTDC IA and reached the lowest value at 24° CA bTDC.

Most of the PCCI studies has focused on changing only IA. However, changing IP and extending ID associated with increased IA may provide advantages. Shi *et al.* [28] injected 45 mg fuel at 40 MPa, 60 MPa, 80 MPa, and 100 MPa IP into the constant volume combustion chamber at 4 MPa and 750 K. An evaporation time was over 3.5 ms for 40 MPa, around 3 ms for 60 MPa, over 2.5 ms for 80 MPa and 2.2 ms at 100 MPa. Du *et al.* [29] changed the IP between 40 MPa and 160 MPa, taking ambient pressure as 4 MPa and 25 mg fuel was injected to constant volume combustion chamber. At the 40 MPa IP, initial combustion center aroused at 20 mm axially and 2 mm radially away from the injector. These values were above 35 mm and 2 mm for 100 MPa pressure. Wall wetting was observed in axial direction at 120 MPa IP, and both axial and radial directions at 160 MPa IP. Wang *et al.* [30] carried out a study and observed an increase in ID nearly 30% when IP decreased from 160-80 MPa. Kiplimo *et al.* [31] manipulated IA between 10° CA bTDC and 30° CA bTDC with 5° CA intervals, IP was 80 MPa and 140 MPa. At 80 MPa IP, with the increase of IA 5° CA, 6° CA, 8.5° CA, 11° CA, and 15° CA ID was observed, respectively. After 20° CA bTDC IA, a certain duration existed between end of injection (EOI) and SOC. Penetration depths were also investigated in the study. After 1° CA from SOI, penetration depth was two times higher at 15° CA bTDC IA and three times at 30° CA bTDC compared to 10° CA bTDC. After 4° CA from SOI, penetration depth became insignificant. Yun *et al.* [32] conducted a study at 3 bar IMEP, between 2° CA bTDC and

34° CA bTDC IA, 700 bar, 1100 bar, and 1500 bar IP. The NO_x increased and reached around 1300 ppm up to 20° CA bTDC IA at 700 bar IP, decreased around to 400 ppm at 25° CA bTDC, and then decreased to 100 ppm at 34° CA bTDC. The PM decreased after 25° CA bTDC IA which is a higher than peak NO_x point. The THC and CO were the smallest at 10° CA bTDC IA, then both emissions increased, especially THC. Also the effect of IP on ID was examined and it was observed that IP was quite determinant factor on the ID at smaller IA. But, after the 25° CA bTDC IA significant ID reductions could not be observed by the changing of IP.

As mentioned earlier, high EGR is applied in most of the PCCI studies. However, the effect of IA can be seen more obviously in studies conducted at low EGR or non-EGR condition. This study conducted non-EGR condition. Decreased IP and increased IA, and reduced fuel pressurization work in order to keep the SOC close to TDC is a logical strategy. For this purpose, in this study, the behaviour of the PCCI strategy was investigated with different IA and IP under a constant speed and constant IFQ. Limited article gave a knowledge about the effect of different IP with non-EGR condition, it is aimed to make a contribution literature on this subject. In addition, few study examines composition of the NO_x formed. The aim of this study is to give a holistic idea and knowledge of the strategy. Besides this, general performance, emission and specific emissions were presented. Moreover, there are so limited studies that specifically examine the EOI temperature. The evaluation of EOI temperature is another novel of the study.

Experimental Set-up and Test Procedure

In this study, TUMOSAN brand, 4-cylinder, turbocharged engine was used. The experiments were carried out at partial load and the turbocharger is not able to provide a constant compressor output pressure under these condition due to low exhaust enthalpy. In order to keep the intake pressure constant, the connection of compressor output and intercooler was disassembled. Specifications of the engine are presented in tab. 1.

Table 1. Engine specifications

Specification	Name/value
Engine model	TUMOSAN S8000 CR
Rated power	84.5 kW (at 2300 rpm)
Maximum torque	405 Nm (at 1500 rpm)
Cylinder number	4
Displacement volume	3.9 liter
Compression ratio	17
İnjection system	Common-rail
Minimum BSFC	217 g/kWh

The engine was braked by AVL INDY s44-2/0934 dynamometer. The IFQ was measured with AVL 735 CME and sensitivity of this device is 0.12%. IA, which commanded by Open-ECU, was checked with Fluke 80i-110s type current clamp. Effective torque was measured by HBM T12HP torque-cell with a 0.01% sensitivity. In-cylinder pressure was evaluated by Kistler 6045B piezoelectric pressure sensor with 0.2% sensitivity. The CO_2, CO, THC, and NO_x were measured by AVL AMA i60 gas analyser, PM was measured with AVL SPC478. Intake air pressure was acquired with BYC MAP sensor, intake air temperature was measured by *K*-type thermocouple, cooling water temperature was regulated by AVL Consyscoll 200 with 1^{o} C accuracy. Air-flow was measured by AVL FSA 100 with 0.8% sensitivity. With the help

of AVL PUMA, IA, IP, IFQ, and engine speed were determined by the Open-ECU principle. Real-time analysis of in-cylinder pressure with respect to crank position was processed with AVL Indicom. The current clamp signal was also evaluated and SOI was precisely confirmed. The test system lay-out is seen at fig. 1.

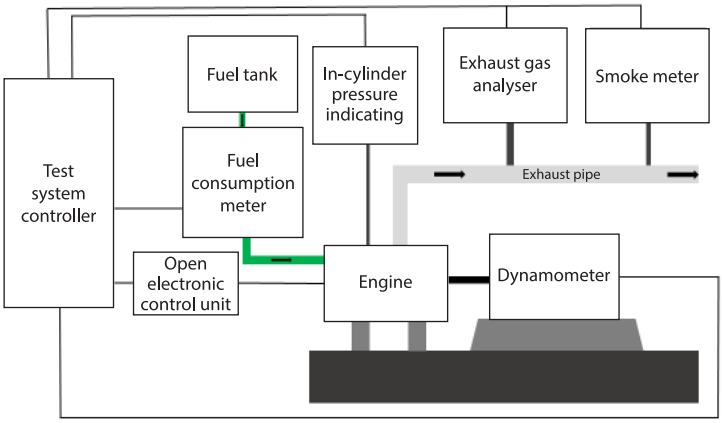

Figure 1. Engine test system lay-out

In order to determine the test points, extensive literature was examined. With the help of these studies, the essentials of injection parameters were determined. This study was carried out at 1500 rpm engine speed and 20 mg per stroke IFQ. At this condition, the air excess ratio was 3.2. The EN590 diesel fuel was used. The intake air pressure was 100.3 kPa, the ambient temperature was 20 °C. Oil pressure was conditioned at 253 kPa and temperature at 84 °C. Cooling water temperature was kept constant at 80 °C. The EGR was by-passed. The IA was varied between 5° CA bTDC and 40° CA bTDC in steps of 5° CA, and the IP was varied between 600 bar and 1400 bar in steps of 200 bar. In order to determine the sensitivity of IA and IP, other parameters were kept constant. The ID, combustion duration, BMEP, IMEP, BMEP/IMEP ratio, maximum in-cylinder pressure, peak in-cylinder temperature, CO, NO_x, THC, and PM, as well as specific equivalents of these emissions were studied. In addition, the NO_2/NO_x ratio, which was absent in most of the studies, was also examined. In the experiments, the engine speed was maintained with a maximum error of 0.08%. For IFQ, this value was around 2% on average, with a peak error is 3.8%. For the IA, mean error value was 0.3%, the highest error was 1%.

As mentioned in the previous paragraph, engine speed and IFQ were constant at all test points. Therefore, the only parameter affecting the injector behaviour during the injection can be practically considered as IP. In addition, the pressure of the environment, which varies with IA, also affects the injection process, but the pressure difference is proportionally very high and this effect is negligible. It is beneficial to know the injection durations. At 600 bar IP, the injection duration is 10.98° CA, at 800 bar IP it is 9.73° CA, at 1000 bar IP it is 9.36° CA, at 1200 bar IP it is 8.5° CA, and at 1400 bar IP it is 8.28° CA.

Results and discussion

In the PCCI strategy, the combustion conditions are extremely important. For this reason, firstly ID and combustion duration values should be examined rather than performance and emission.

Figure 2 shows ID values at different IP and IA. The ID was calculated based on 5% total heat release. As expected, when IA increased, ID increased progressively. But at 5° CA bTDC and 10° CA bTDC IA, a different trend was observed. When IA increased from 5° CA bTDC to 10° CA bTDC, ID got shortener in some samples and then started to increase. This was due to the occurrence of modulated kinetic combustion regime, another LTC strategy, at 5° CA bTDC IA. In this IA, SOC was shifted to after TDC and therefore, ID was prolonged. At 15° CA bTDC IA, SOC revealed before TDC at high IP, while at 600 bar and 800 bar IP SOC revealed after TDC. At 20° CA bTDC IA and above, combustion started before TDC at all IP. At higher IA, the SOC tended to be close because ID increased excessively. This trend was more pronounced at higher IP. It is important to understand the interpretation of IA and ID together with EOI. If there is a positive dwell angle between EOI and SOC, all of the fuel is injected into the cylinder before SOC. Analysing the SOI, ID and EOI data, it was seen that there was a positive dwell angle between EOI and SOC in all samples. Of course, as the AI increased, the difference between these two values became bigger. At the PCCI region the ID was generally longer at higher IP. The injection was completed in a shorter duration at these IP, which also had a partial effect on this. If the analysis was done in terms of IP, lower IP caused longer ID at small IA. After 20° CA bTDC IA, character change was seen, but 600 bar IP serial was an exceptional case. Then, the increase in IA also led to a greater ID at higher IP. This can be explained by the fact that the better pulverized fuel was more spread in the combustion chamber, improving the macro mixture and improving the lean mixture characteristics. In order to verify this assertion, the combustion duration in this range have to be relatively long.

As mentioned in the previous paragraph, combustion duration is as important as ID in PCCI. Because the strategy is based on creating a dilute mixture and extending the combustion duration. Actually, the longer ID is in order to longer combustion duration. In the study, the period between 5% total heat release and 90% total heat release was assumed as the combustion duration. As can be seen from fig. 3, combustion duration was shorter at lower IA. In the PCCI region, it was observed that combustion generally takes longer duration. From the previous paragraph, it was predicted that combustion duration was expected to increase at higher IA and IP values. It can be seen from the results, at higher IP in the relevant range, fuel was mixed with extended effective air volume, so increasing the dilute characteristic and decreasing the combustion rate. At 600 bar and 800 bar IP, the expected combustion duration values were not

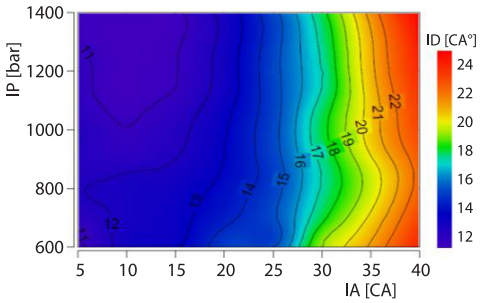

Figure 2. Variation of ignition delay depending on IP and IA

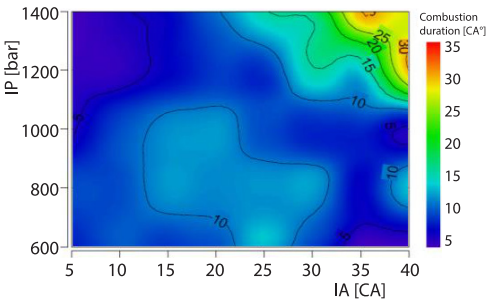

Figure 3. Variation of combustion duration depending on IP and IA

observed depending on the increase in IA. This can be attributed to many factors. The main factor could be the high Sauter mean diameter caused by the low IP and the delayed break-up. Mixture homogeneity was insufficient under these conditions. But a significant decrease was achieved at higher IP. In parallel with this, peak in-cylinder pressure values are expected to increase in this range. As can be seen from the comments, made in the following evaluations and results, supported this hypothesis.

The IP not only changes the injected fuel pressurization work, but also affects ID and state of atomization. Therefore, working with low IP and high IA are matter of interest. Figure 4 shows the BMEP at different IP and IA. At the 5° CA bTDC IA, SOC shifted to expansion, so BMEP values were low. As IA increased, BMEP increased and maximum BMEP was obtained between 10° CA bTDC and 20° CA bTDC IA for each IP. After 15°-20° CA bTDC IA at high IP, BMEP took values outside of acceptable limits, in this working conditions BMEP decreased significantly. It is because combustionok place mostly before TDC or combustion duration was so prolonged. If SOC starts earlier than nominal condition, thermal losses increase. Increased thermal losses can be considered as one of the reasons of BMEP reduction at excessive IA. Srivatsa *et al.* [33] showed that exhaust gas temperatures increased at greater IA. This is another factor explaining the decrease in BMEP. If IA increase excessively, atomization capability decreases per unit time, so ID increases. The decrease in IP also affects negatively fuel atomization process and prolongs ID. It is seen that working with lower IP gave better results in terms of BMEP at relatively high IA or PCCI region. This is due to the wall wetting tendency at higher IP. At 1400 bar IP, the highest BMEP emerged at 10° CA bTDC IA, followed a very rapid decrease with increasing of IA. Similar trends were observed at 1200 bar and 1000 bar IP with lower gradient. Higher BMEP values were observed at high IA at the 800 bar and 600 bar IP series, compared to other IP. Maximum BMEP was observed at 15° CA bTDC IA for 800 bar IP and at 20° CA bTDC IA for 600 bar IP. On the other hand, after the peak BMEP was attained, the decrease in BMEP was slower at lower IP when the IA increased. Because fuel pressurization work decreased and the impingement risk was lower.

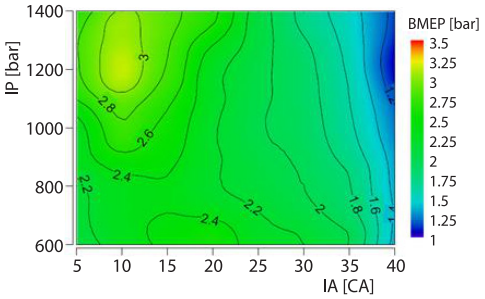

Figure 4. Variation of BMEP depending on IP and IA

Working at the 600 bar IP was an advantage of 17% at 25° CA bTDC IA, 19% at 30° CA bTDC, and 24% at 35° CA bTDC compared to 1400 bar IP in terms of BMEP. At high IP, when IA increased, BMEP drop rate was an increase of up to three times compared to the highest BMEP point. However, it is a mistake that only factor is early SOC as a result of reduced ID with increasing IP. Here, fuel overflowing rate from the piston cavity increased because of early injection when the atomization ability was low.

Combustion conditions change with varying IP and IA. These manipulations affect SOC point and burn rate. Therefore, temperatures and pressures during combustion vary. Instantaneous friction force effects BMEP, especially in the ring-cylinder interaction, hence it is useful to use indicated parameters to examine effects of the combustion event. Figure 5 shows IMEP values. In the IMEP results, generally, the amount of change which was obtained at different IA for each IP was smaller than BMEP difference. In this study, the IFQ is far from the high load. The high ratio of mechanical losses in indicated work for this case explains the different trend between IMEP and BMEP. Particularly at low IP, relatively smaller changes oc-

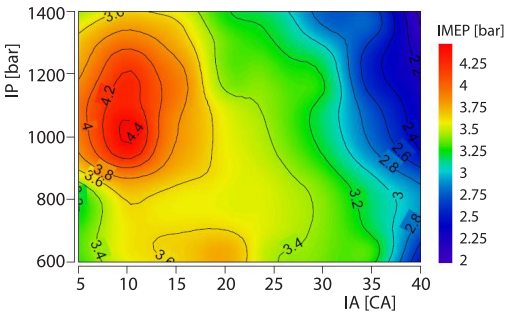

Figure 5. Variation of IMEP depending on IP and IA

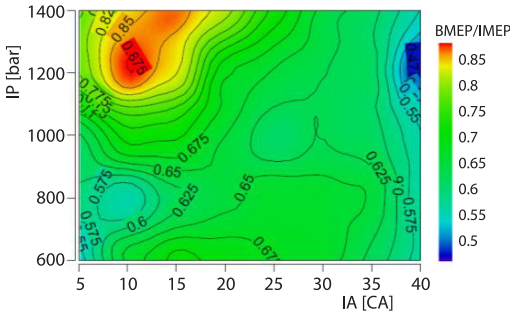

Figure 6. The BMEP/IMEP ratio depending on IP and IA

curred in IMEP, when IA changed, than BMEP. A slower change in IMEP compared to BMEP was observed, especially at IA higher than the IA at which the maximum BMEP or IMEP was obtained. This was more evident for 600 bar and 800 bar IP. Especially, very close values with minor variations were observed after the maximum IMEP point at 15° CA bTDC IA. Also, at higher IP and these IA, a slower downward trend emerged than BMEP. Although the combustion started earlier, relatively small change observed here by virtue of slower flame propagation. At higher IP series, the difference between IMEP and BMEP increased numerically. In this region, the variation of BMEP increased at different IA. This difference was particularly pronounced under CDC regime (relatively short ID and high temperature combustion region). As a general trend, the difference between IMEP and BMEP were greater for higher IA. Especially at high IP values, this difference was more apparent. In addition the aforementioned factors afore, SOC location also strongly effects to this. At this region, SOC occurred with a higher advance from the TDC than in other cases. This increases the in-cylinder pressure that the piston has to overcome until it reaches to TDC. This increases the amount of work which has to be supplied from flywheel to the system in the compression stroke and consequently the mechanical efficiency decreases. Figure 6 is presented to better demonstrate the trends and comparisons of IMEP and BMEP. Figure 6 indicates the BMEP/IMEP ratios. In parallel with the comments made previously, it could be seen from the graph that the BMEP/IMEP ratio in the LTC regionok lower values.

As it is seen from fig. 7, peak in-cylinder pressure was bigger at higher IA and lower IP. At 1400 bar IP, the peak in-cylinder pressure reached its highest value at 15° CA bTDC IA, then decreased until 25 ° CA bTDC IA and after this point remained nearly constant. At 1200 bar IP, small fluctuation occurred between 15° CA bTDC and 35° CA bTDC IA. At 1000 bar IP, the peak in-cylinder pressure increased until 30° CA bTDC IA. At 800 bar and 600 bar IP, the peak in-cylinder pressure increased until 35° CA bTDC IA. At higher IP up to 20° CA bTDC IA performed greater peak in-cylinder pressure, but character change was observed at higher IA and higher peak in-cylinder pressure was observed at lower IP. This could be explained by the fact that at low IA, the ID duration decreased while the IP increased and the peak in-cylinder pressure was reached at closer to TDC. At higher IA and low IP, both the ID duration increased and the quantity of fuel burned in the pre-mixed combustion phase increased, thus the peak in-cylinder pressure increased. In some of the results, the approximate peak in-cylinder pressures were observed, in spite of the different IA. Due to the prolongation of the ID as a result of the increased IA for different IP. Thus, SOI occurred at similar points with similar atomization characteristics. Although this inference can't be made directly, the

fact that there are no significant differences in the effective power values at the related points supports this argument.

In all LTC applications, the temperature in the combustion chamber has great importance. The LTC strategies are constructed with the aim of reducing exhaust emissions and these emissions are strongly affected by the peak in-cylinder temperature. As mentioned before, NO_x emissions increase significantly with increasing in-cylinder peak temperature. One of the main focus of the study is to reduce NO_x. For this reason, the peak combustion temperature shown on fig. 8. has a significant importance. At low IP, the peak combustion temperature was increased in general, when IA increased. At 600 bar and 800 bar IP, peak combustion temperature was reached at 35° CA bTDC IA. At higher IP, the peak combustion temperature was observed at smaller IA. The peak combustion temperature was low under conditions where SOC shifted to expansion. In the regions dominated by the PCCI strategy, in other words, where combustion duration and ID took higher values, the peak combustion temperature was low. As a general trend, fig. 8. gives important insight into the resulting NO_x emissions. However, the same graphs cannot be obtained exactly. Because not only the peak combustion temperature is important, but also where this temperature is reached is quite important. The duration in high temperature zone has a direct effect on NO_x formation. Therefore, an analogy can be drawn between the results of the two graphs, but differences will be observed.

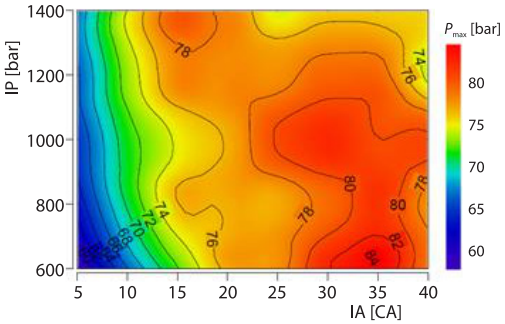

Figure 7. Variation of peak in-cylinder pressure depending on IP and IA

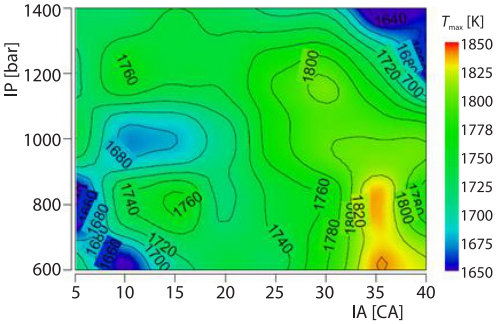

Figure 8. Variation of peak combustion temperature depending on IP and IA

Figure 9 presents NO_x in ppm. As is known, as SOC moves away from the TDC, NO_x increases up to a certain IA where maximum BMEP is achieved. Then NO_x decreases if operating at partial loads, which makes PCCI reasonable. At low IA, higher IP caused higher NO_x, this trend started to change at the 20°-25° CA bTDC IA. This increasing tendency was due to shorter ID and dominant diffusion flame phase, resulting higher flame temperatures, increasing mixture heterogeneity, and increasing cold region in the combustion chamber. At high IA, as a result of increase in mixture homogeneity, a leaner mixture was achieved and flame temperature decreased. Thus, NO_x tended to decrease. The highest NO_x was observed at 20° CA bTDC IA for 1400 bar IP, 25° CA for 1200 bar and 1000 bar IP, 30° CA for 800 bar and 600 bar IP. An important result is NO_x decreased with a higher gradient at lower IP when IA increased after the highest NO_x observed point. This rapid decreasing trend is also seen in the study of Horibe *et al.* [25]. However, relatively low IP led to the highest NO_x at 25° CA bTDC IA and above. This is probably due to local mixture heterogeneity in the zones participating the combustion, droplet break-up, and insufficient macro-mixture formation (in spite of long ID).

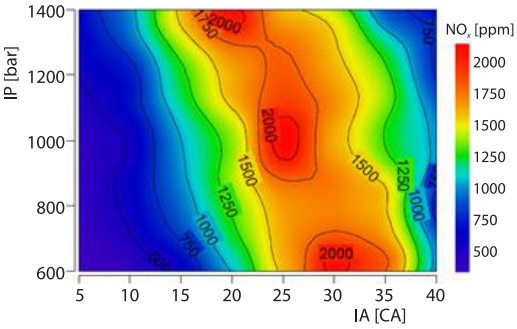

Figure 9. Variation of NOx emission depending on IP and IA

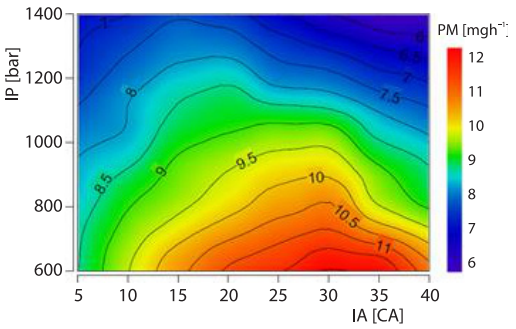

Figure 10. Variation of PM emission depending on IP and IA

The PM emissions in mg per hour unit are presented in fig. 10. According to results, when IA increased, PM initially increased at all IP, then decreasing was observed. At 5° CA bTDC IA, although ambient temperature is quite high when injection started, SOC shifted to expansion. Since the fuel remained in this high temperature zone for an insufficient period, the heat transfer per unit mass was not enough. In this way, it took longer for the appropriate mixture ratio reach the auto ignition temperature. Because expansion has already started and in-cylinder temperatures have started to fall before the SOC, a high ID was obtained. Then as the IA increased up to a certain value, diffusive flame phase became more pronounced while premixed combustion characteristic was suppressed. At the same time, the fact that last fuel particles injected into the cylinder did not have enough time to create a good mixture also triggered this trend. As a result, when IA increased, both the duration taken for fuel particles to vaporize during ID and reach the auto-ignition temperature increased and fuel particles reached a higher penetration depth at lower ambient pressure. Depending on these factors, PM performed a downward trend. At 1400 bar IP, the highest PM occurred at 15° CA bTDC IA, at 1200 bar IP at 20° CA bTDC, and at lower IP at 30° CA bTDC. In addition, working with a higher IP at each IA gave better result. High gradient changed of NO_x could not be observed in PM. The variation in PM that caused by change in IA occurred more slightly. As IP increases, PM decrease is expected depending on the better pulverization. The most dominant factor affecting PM formation is mixture homogeneity rather than temperature. However, the temperature in the injection environment affects the homogeneity of the macro-mixture. Hence, SOI and EOI temperatures are important for mixture formation. There are very few studies including this data. In this study, it was also investigated how SOI and EOI temperature affect PM emission. As can be seen from fig. 10, PM emission variation at 800 bar IP had significant differences. The PM decreased after 30° CA bTDC IA at 800 bar IP. The SOI and EOI temperatures at these IA were calculated as follows. At 30° CA bTDC IA SOI temperature is 767 K and EOI temperature is 851 K, at 35° CA bTDC IA SOI temperature is 720 K and EOI temperature is 802 K, at 40° CA bTDC IA SOI temperature is 684 K and EOI temperature is 761 K. The PCCI is dominant at these IA's. Under these conditions, as IA increased, SOI and EOI temperature decreased as well as the difference between two values increased. The decrease in SOI and EOI temperature led to a decrease in the heat flux to the fuel during this process. This led to an increase in the ID. The 35° CA bTDC IA was chosen to examine the SOI and EOI depending on the IP variation. At 35° CA bTDC IA, the SOI was calculated as 720 K. At 600 bar IP, EOI temperature was 808 K, at 800 bar IP EOI temperature was 802.3 K, at 1000 bar IP EOI temperature was

797 K, at 1200 bar IP EOI temperature was 795 K, at 1400 bar IP EOI temperature was 791 K. At this IA, PM emission decreased significantly as IP increased. The main factor in this decrease is the reduction of local oxygen starvation due to improved pulverization. Ambient temperature affects this process. Therefore, besides the main effect of IP, SOI, and EIO temperature should be considered as a secondary parameter. Considering these two factors, with increasing IP at constant IA, both the mixture homogeneity in terms of fluid mechanics increased and the mixing duration increased due to the lower EOI temperature. The decrease in PM as IP increases can be explained by these two factors.

The CO in ppm is shown in fig. 11. There was no significant change in CO until the IA was increased up to 20° CA bTDC. Besides CO was largely independent of IP at these IA. After 25° CA bTDC IA, the differences became more visible, after this point both sensitivity of the IA and IP was quite high. Especially, at 35° CA bTDC IA and afterward, serious increase was observed in CO, and working at higher IP caused higher CO. At 1400 bar IP, differences increased to approximately 3.3 times at 30° CA bTDC IA and 13.1 times at 40° CA bTDC compared to 20° CA bTDC. At 600 bar IP, these values were approximately 2.1 and 12.3, respectively. CO formation in Diesel engines is highly dependent on the lazy flame and an increase of CO is expected in the PCCI. It can be said that CO increased as a result of the air-fuel mixture occupied a larger volume in the cylinder with increasing IP. Thus leaner zones increased proportionally and flame temperatures decreased in these zones. This is also associated with an increase in CO with increasing IA. There was a 75% difference between the lowest and the highest IP at 30° CA bTDC IA, this difference increased to 400% at 35° CA bTDC. This confirms the CO increase hypothesis. The CO increased owing to too long ID at these IA and more dilute mixture combustion. At the 40° CA bTDC IA, Ratio of differences reduced to a lower level, but emission values increased. The lowest and highest CO differed as 36% at this IA. Low in-cylinder temperature during the injection at this range affected the atomization regime negatively. Moreover, effect of IP began to obscure.

THC showed a similar trend with CO, as can be seen in fig. 12. Significant differences in THC for different IA occurred after 20° CA bTDC IA. It was observed that IP had no serious effect on THC up to 30° CA bTDC IA. The effect of IP on THC was more limited, especially when compared to other emissions. From this point of view, it is concluded that the IP effect became visible later than IA effect in terms of THC. At 1400 bar IP 1.34 times higher THC was observed at 30° CA bTDC IA, 2.15 times higher at 35° CA, and 6.26 times higher at 40° CA with compared to 20° CA IA. At 600 bar IP, these values were 1.68, 2.86, and 5.32, respectively. Although it is not clear from the scaling on the counter map, significant IP dependent differences were observed at the 40° CA bTDC IA. At 40° CA bTDC IA, 1400 bar IP conditions emitted

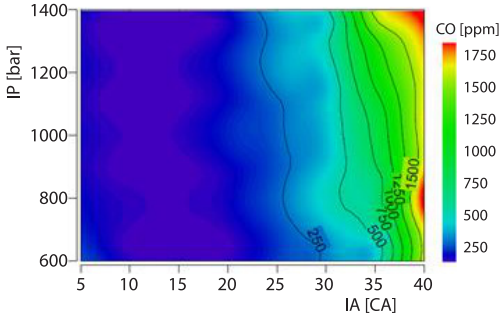

Figure 11. Variation of CO emission depending on IP and IA

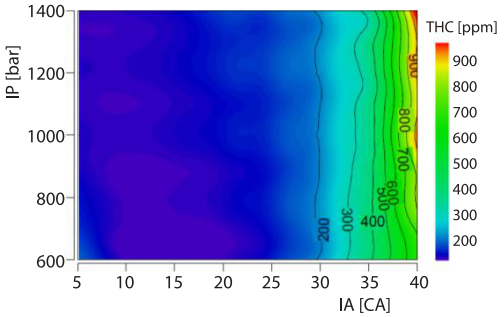

Figure 12. Variation of THC emission depending on IP and IA

51% more THC compared to 600 bar IP. This situation occurred as a result of the relatively low pressure environment of the combustion chamber, the fact that the fuel wasn't able to stagnate while mixing with the air and hitting the piston's upper surface or cylinder walls. The dramatic increase in high IA values of THC in the PCCI strategy can be explained by wall wetting [34].

Nitrogen and oxygen compounds are called as NO_x as a community name. However, each NO_x component effects the environment at different scale. Most of the NO_x formed in internal combustion engine is composed of NO. Another important NO_x is NO_2. In gasoline engines, approximately 2% of NO_x is NO_2. This value may vary depending on operating conditions and in some cases this value may be slightly higher. In Diesel engines, 5-20% of NO_x is NO_2. The ratio of NO_2 to NO_x increases as engine speed increases and engine load decreases. NO_2 is essentially an intermediate reaction in the formation of NO, shorter reaction time results higher NO_2/NO_x ratio, because the reaction rate is insufficient for conversion NO. In addition, relatively low combustion temperature and rapid cooling rate after the combustion at low engine load also trigger NO_2 formation. When PCCI studies are surveyed, it is very difficult to find information about NO_2/NO_x ratio. Increase in pre-mixing ratio, decrease in combustion rate, decrease in combustion temperature, and decreasing in cold zones in the combustion chamber in PCCI strategy arouse curiosity about what the NO_2/NO_x ratio will be. Figure 13 shows NO/NO_x ratios under different IA and IP. The NO_x is practically composed of NO and NO_2. However, trace amounts of other NO_x compounds such as N_2O, and N_2O_5 are also observed. Although these trace NO_x components do not create significant variety of percentage, NO/NO_x ratios are presented in order to avoid theoretical lapse. It was observed that NO/NO_x ratio increased initially and then decreased when IA increased at low IP. Although there was no continuous trend at higher IP, similar trending results emerged. At the CDC region, high IP gives a higher NO/NO_x ratio and lower NO_2/NO_x. In this study, NO/NO_x ratios at 20°-25° CA bTDC IA, which can be called the PCCI transition zone, were relatively close to each other. Afterwards, NO/NO_x decreased with increasing IA, thus NO_2/NO_x ratio increased. In the PCCI region, NO/NO_x ratio decreases and NO_2/NO_x ratio increases as the IA increases due to the decrease in flame speed and the decrease in combustion chamber temperatures.

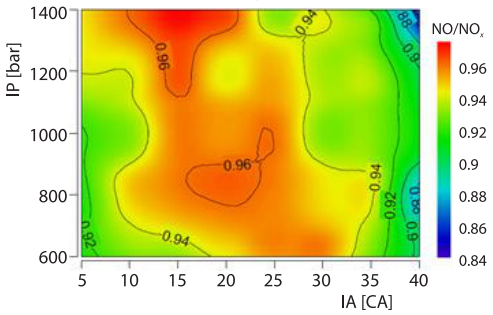

Figure 13. Variation of NO/NO_x ratio depending on IP and IA

Volumetric concentration emission value gives information about net amount of emitted emission environment, but this is insufficient, because it does not give any idea about the emission per unit power. For this reason, specific emissions are given in figs 14-17. In this way, it is possible to make a more meaningful assessment by having information about the emissions per unit power.

In terms of general framework of PCCI principle, the most important graph is fig. 14, which shows specific NO_x. According to results, working at low IP up to 25° CA bTDC IA performed lower specific NO_x. Specific NO_x under 1400 bar IP at 10° CA bTDC IA is 1.8 times higher than 600 bar IP at the same IA. Up to 20° CA bTDC IA, this trend was approximately maintained and two times higher specific NO_x was obtained. Around the 25°-30° CA bTDC IA, the relation between these variables became more complex and trend changed. After this, higher IP caused lower specific NO_x. However, at 40° CA bTDC IA, changing trend started to diverge again with the power decrease due to impingement caused by higher IP. For a conven-

tional diesel engine, 35° CA IA is sufficient to cause serious impingement, which is supported by [34]. In 25°-35° CA bTDC IA range, where PCCI strategy gave relatively reasonable results, operating with higher IP produced lower specific NO_x. Another reason was NO_x decreasing in ppm or g per hour after 20° CA bTDC IA at high IP and 30° CA bTDC at low IP. Regardless of IP, it was seen that specific NO_x increased up to the highest NO_x point in ppm when only IA is taken into account. However, NO_x in ppm entered a downward trend earlier. It is because, depending on IA, maximum power at the related IP was achieved earlier and power tended to decrease less in the investigation area. Thus, specific NO_x tended to decrease with a little delay than NO_x in ppm.

Figure 15 shows the specific PM. Specific PM increased as IA increased in each IP, apart from exceptional cases. In the whole data set, only a significant decrease occurred when shifting to 10° CA bTDC IA at 1000 bar IP and to 35° CA bTDC at 800 bar IP. A low trend of changing in PM was seen in fig. 15. Figure 15 showed that, when IA increased, specific PM increased as well. Over a certain IA, PM can increase, as seen with Jung *et al.* [35]. In the data set of this study, it was observed that desired specific PM reduction could not be achieved.

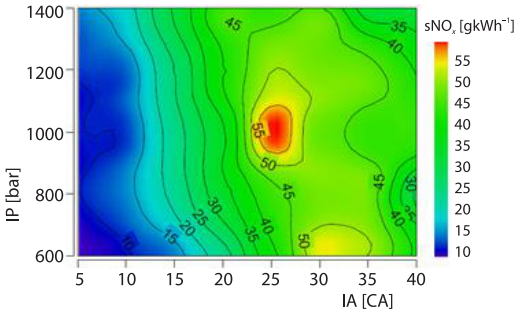

Figure 14. Variation of specific NO_x emission depending on IP and IA

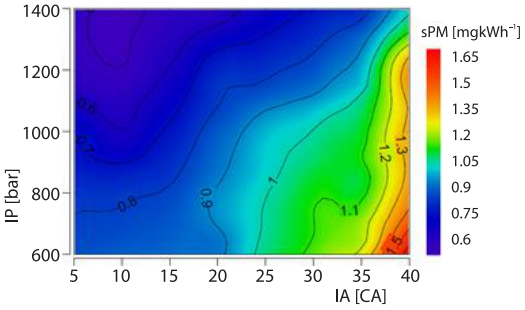

Figure 15. Variation of specific PM emission depending on IP and IA

According to the fig. 16, specific CO emissions were close to each other until 20° CA bTDC IA, similar to CO in ppm. The differences became visible at 25° CA bTDC IA. At 30° CA bTDC IA, differences up to 2.1 times occurred between the lowest and highest IP, and at 40° CA bTDC IA, differences occurred as 1.8 times. The CO difference in ppm unit was not so high relatively. Higher differences have emerged due to decreasing of effective power at high IA. Dramatic specific CO increment at lower IP occurred at higher IA. At 600 bar IP, there were no dramatic increases up to 35° CA bTDC IA. At 800 bar and 1000 bar IP, acceptable differences occurred up to 35° CA bTDC IA. At these IP, the maximum power appeared at higher IA. In

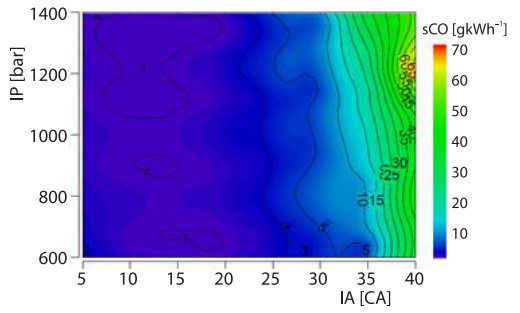

Figure 16. Variation of specific CO emission depending on IP and IA

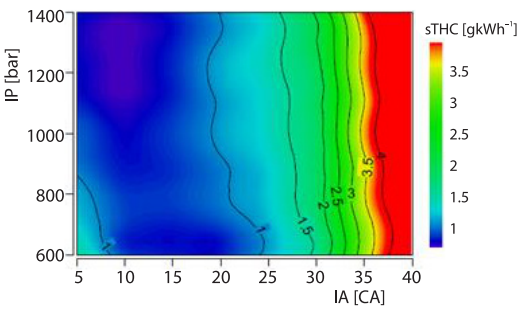

Figure 17. Variation of specific THC emission depending on IP and IA

addition, effective power drop gradient after this point was relatively smaller. These two factors can be explained as the reason for this situation.

As can be seen in fig. 17, specific THC and specific CO were similar. Significant differences in specific THC for IA and IP appeared at larger IA like 30° CA bTDC. However, up to 35° CA bTDC IA, there was no significant change depending on IP while dramatic differences appeared at 40° CA bTDC IA.

Conclusions

It was observed that at high IP, after the highest BMEP was obtained, the decrease in BMEP was faster when the increase in IA. At low IP, it was observed that the change with increasing IA remained at more acceptable levels. Therefore, it can be concluded that working with lower IP in the PCCI operating region is more reasonable in terms of BMEP. In this study, it was observed that above 35° CA bTDC IA produced unacceptable values in terms of performance. It can be deduced that the dramatic losses at high IA can be explained by not only the deterioration of combustion, but also by the increase in the proportion of fuel that cannot participate in combustion as a result of impingement. This is more evident at high IP. The decrease in peak in-cylinder pressure value for all IP above 35° CA bTDC IA supports this conclusion. At the high IA and low IP, it was observed that the maximum in-cylinder pressure values were higher, although they did not contribute positively to effective power output. The decrease in IMEP was more acceptable than the decrease in BMEP as moving to the PCCI region.

When emissions were analysed, it was observed that CO and THC in ppm showed similar trends. The CO and THC were not significantly affected of the increase in IA and IP at the beginning practically. But these two emissions started to increase when moving to PCCI zone. In this range, IP effected both emissions more than IA. For both emissions, the effect of IA became more visible than IP. At low IA, higher NO_x was observed as the IP increased. Then, as the mixture heterogeneity decreased and moved into the PCCI region, NO_x also decreased due to a decrease in flame temperature. After reaching peak NO_x at low IP, NO_x decreased with a larger gradient as IA increased. However, low IP in the selected range produced higher NO_x values in the PCCI region and it was found that it was inconvenient to operate below a certain IP value. In addition, while CDC gave lower NO_2/NO_x ratios, NO_2/NO_x ratios increased in PCCI region. For PM, higher IP resulted in lower PM without exception. As the IA increased above a certain value, PM decreased but not do desired levels.

If the obtained data was analysed in terms of specific emissions, specific CO was similar with ppm values and changing trends. It is possible to make a similar interpretation for specific THC as for specific CO. In CDC region, lower IP caused in lower specific NO_x, whereas in PCCI region, lower IP resulted in higher specific NO_x. In this study, the desired level of PM reduction in g per hour was not reached and the PM reduction remained weak. As a result, the specific PM reduction, one of the main objectives of the PCCI strategy, was not achieved.

Nomenclature

Acronyms

aTDC – after top dead center
BMEP – brake mean effective pressure
bTDC – bottom top dead center
BTE – brake thermal efficiency
CDC – conventional diesel combustion
EGR – exhaust gas re-circulation
EOI – end of injection
HCCI – homogenous charge compression ignition
IA – injection advance
ID – ignition delay
IFQ – injected fuel quantity
IMEP – indicated mean effective pressure
IP – injection pressure
LTC – low temperature combustion
PCCI – pre-mixed charge compression ignition

PM – particulate matter
RCCI – reactivity charge compression ignition
SOC – start of combustion
SOI – start of injection
TDC – top dead centre
THC – unburned hydrocarbon

References

[1] Ozer, S., *et al*., Experimental Investigation of the Effect of the Use of Nanoparticle Additional Biodiesel on Fuel Consumption and Exhaust Emissions in Tractor Using a Coated Engine, *Thermal Science*, *27* (2023), 4B, pp. 3189-3197
[2] Imtenan, S., *et al.*, Impact of Low Temperature Combustion Attaining Strategies on Diesel Engine Emissions for Diesel and Biodiesels: A Review, *Energy Conversion and Management*, *80* (2014), Apr., pp. 329-356
[3] Huang, H., *et al*., Comparative Study of Effects of Pilot Injection and Fuel Properties on Low Temperature Combustion in Diesel Engine Under a Medium EGR Rate, *Applied Energy*, *179* (2016), Oct., pp. 1194-1208
[4] Rangasamy, M., *et al*., Impact of Operating Parameters on on Energy Efficiency and Regulated Emissions of Dual fuel Direct Injected Reactivity Controlled Compression Ignition Combustion, Energy Sources – Part A: *Recovery, Utilization, and Environmental Effects*, On-line first, https://doi.org/10.1080/15567036.2021.1919791, 2021
[5] Zhu, H., *et al*., Effect of Biodiesel and Ethanol on Load Limits of High-Efficiency Premixed Low Temperature Combustion in a Diesel Engine, *Fuel*, *106* (2013), Apr., pp. 773-778
[6] Xu, G., *et al.*, Multi-Objective Optimization of the Combustion of a Heavy-Duty Diesel Engine with Low Temperature Combustion under a Wide Load Range: (I) Computational Method and Optimization Results, *Energy*, *126* (2017), May, pp. 707-719
[7] Jain, A., *et al*., Effect of Split Fuel Injection and EGR on NO_x and PM Emission Reduction in a Low Temperature Combustion (LTC) Mode Diesel Engine, *Energy*, *122* (2017), Mar., pp. 249-264
[8] Bobi, S., *et al*., Combustion and Emission Control Strategies for Partially-Premixed Charge Compression Ignition Engines: A Review, *Fuel*, *310* (2022), 122272
[9] Doll, U., *et al*., Impact of a Split Injection Strategy on Mixing, Ignition and Combustion Behavior in Premixed Charge Compression Ignition Combustion, *Fuel*, *294* (2021), 120511
[10] Sun, C., *et al*., Impact of Fuel and Injection Timing on Partially Premixed Charge Compression Ignition Combustion, *Energy and Fuels*, *30* (2016), 5, pp. 4331-4345
[11] Torregrosa, A. J., *et al*., Impact of Gasoline and Diesel Blends on Combustion Noise and Pollutant Emissions in Premixed Charge Compression Ignition Engines, *Energy*, *137* (2017), Oct., pp. 58-68
[12] Murcak, A., *et al.*, Effect of Injection Timing to Performance of a Diesel Engine Fuelled with Different Diesel-Ethanol Mixtures, *Fuel*, *153* (2015), Aug., pp. 569-577
[13] Bhave, N. A., *et al*., Effect of Brown's Gas Addition on Combustion and Emissions of Homogeneous Charge Compression Ignition Engine, Energy Sources – Part A: *Recovery, Utilization, and Environmental Effects*, On-line first, https://doi.org/10.1080/15567036.2020.1817194, 2020
[14] Sankaralingam, R. K., *et al*., Experimental Studies on Premixed Charge and Reactivity-Controlled Compression Ignition Combustion Modes Using Gasoline/Diesel Fuel Combination, *Case Studies in Thermal Engineering*, *39* (2022), 102467
[15] Qiu, L., *et al.*, Partially Premixed Combustion Based on Different Injection Strategies in a Light-Duty Diesel Engine, *Energy*, *96* (2016), Feb., pp. 155-165
[16] Liu, H., *et al*., Study of the Control Strategies on Soot Reduction Under Early-Injection Conditions on a Diesel Engine, *Fuel*, *139* (2015), Jan., pp. 472-481
[17] Wei, M., *et al*., Effects of Injection Timing on Combustion and Emissions in a Diesel Engine Fueled with 2, 5-Dimethylfuran-Diesel Blends, *Fuel*, *192* (2017), Mar., pp. 208-217
[18] Kim, K., *et al*., Control Strategy of Mode Transition Between Low-Temperature Combustion and Conventional Combustion in a Light-Duty Diesel Engine, *IFAC Proceedings Volumes*, *46* (2013), 21, pp. 723-729
[19] Parks II, J. E., *et al.*, Emissions from Premixed Charge Compression Ignition (PCCI) Combustion and Affect on Emission Control Devices, *Catalysis Today*, *151* (2010), 3-4, pp. 278-284
[20] Liu, B., *et al*., Experimental Investigation of Injection Strategies on Particle Emission Characteristics of Partially-Premixed Low Temperature Combustion Mode, *Applied Thermal Engineering*, *141* (2018), Aug., pp. 90-100
[21] Rohani, B., *et al*., Effect of Injection Strategy on Smoothness, Emissions and Soot Characteristics of PCCI-Conventional Diesel Mode Transition, *Applied Thermal Engineering*, *93* (2016), Jan., pp. 1033-1042

[22] Qian, Y., *et al*., Experimental Studies on the Key Parameters Controlling the Combustion and Emission in Premixed Charge compression Ignition Concept Based on Diesel Surrogates, *Applied Energy*, *235* (2019), Feb., pp. 233-246
[23] Pandey, S.K., *et al.*, Potential of Early Direct Injection (EDI) for Simultaneous NOx and Soot Emission Reduction in a Heavy Duty Turbocharged Diesel Engine, *Applied Thermal Engineering*, *158* (2019), 113762
[24] Li, T., *et al*., Effect of Two-Stage Injection on Unburned Hydrocarbon and Carbon Monoxide Emissions in Smokeless Low-Temperature Diesel Combustion with Ultra-High Exhaust Gas Re-Circulation, *International Journal of Engine Research*, *11* (2010), 5, pp. 345-354
[25] Horibe, N., *et al.*, Selection of Injection Parameters for Various Engine Speeds in PCCI-Based Diesel Combustion with Multiple Injection, SAE Technical Paper, 2011-01-1822, 2011
[26] Pandey, S., *et al*., Investigation of Fumigation of Ethanol and Exhaust Gas Re-circulation on Combustion and Emission Characteristics of Partially Premixed Charge Compression-Ignition Engine, Energy Sources – Part A: *Recovery, Utilization, and Environmental Effects*,On-line first, https://doi.org/10.1080/15567036.2020.1868625, 2020
[27] Park, S., *et al*., Effects of Various Split Injection Strategies on Combustion and Emissions Characteristics in a Single-Cylinder Diesel Engine, *Applied Thermal Engineering*, *140* (2018), July, pp. 422-431
[28] Shi, Z., *et al.*, Effect of Injection Pressure on the Impinging Spray and Ignition Characteristics of the Heavy-Duty Diesel Engine Under Low-Temperature Conditions, *Applied Energy*, *262* (2020), 114552
[29] Du, W., *et al.*, Effects of Injection Pressure on Ignition and Combustion Characteristics of Impinging Diesel Spray, *Applied Energy*, *226* (2018), Sept., pp. 1163-1168
[30] Wang, D., Energy Conversion and Combustion Characteristics of Diesel and N-Alcohol Blends (N-Propanol to N-Hexanol) under Low Ambient Temperature and Different Injection Pressures, *Combustion Science and Technology*,)n-line first, https://doi.org/10.1080/00102202.2023.2270626, 2023
[31] Kiplimo, R., *et al.*, Effects of Injection Pressure, Timing and EGR on Combustion and Emissions Characteristics of Diesel PCCI Engine, SAE Technical Paper, 2011-01-1769, 2011
[32] [Musculus, M. P., On the Correlation Between NO_x Emissions and the Diesel Premixed Burn, SAE Technical Paper, 2024-03-08, 2024
[33] Srivatsa, C.V., *et al*., Exploring the Possibility of Achieving Partially Premixed Charge Compression Ignition Combustion of Biodiesel in Comparison Ultra Low Sulfur Diesel on a High Compression Ratio Engine, *Combustion Science and Technology*, *195* (2023), 4, pp. 746-777
[34] Lu, Y., Su, W., Effects of the Injection Parameters on the Premixed Charge Compression Ignition Combustion and the Emissions in a Heavy-Duty Diesel Engine, Proceedings of the Institution of Mechanical Engineers – Part D: *Journal of Automobile Engineering, 231* (2017), 7, pp. 915-926
[35] Jung, Y., *et al.*, Premixed Compression Ignition Combustion with Various Injector Configurations in a Heavy Duty Diesel Engine, Proceedings of the Institution of Mechanical Engineers – Part D: *Journal of Automobile Engineering, 227* (2013), 3, pp. 422-432

Paper submitted: January 5, 2024
Paper revised: May 20, 2024
Paper accepted: May 23, 2024